Acta Crystallographica Section D
Biological Crystallography
ISSN 0907-4449

Structure of the phenylhydrazine adduct of the quinohemoprotein amine dehydrogenase from *Paracoccus denitrificans* at 1.7 Å resolution

Saumen Datta,[a]† Tokuji Ikeda,[b] Kenji Kano[b] and F. Scott Mathews[a]*

[a]Washington University School of Medicine, St Louis, MO 63110, USA, and [b]Kyoto University, Sakyo-ku, Kyoto 606-8502, Japan

† Present Address: Department of Biochemistry, Johns Hopkins School of Medicine, Mudd Hall 247, 3400 North Charles Street, Baltimore, MD 21218, USA.

Correspondence e-mail: mathews@biochem.wustl.edu

Received 6 May 2003
Accepted 25 June 2003

PDB Reference: quinohemoprotein amine dehydrogenase phenylhydrazine adduct, 1pby, r1pbysf.

The 109 kDa quinohemoprotein amine dehydrogenase (QHNDH) from *Paracoccus denitrificans* contains a novel redox cofactor, cysteine tryptophylquinone (CTQ). This cofactor is derived from a pair of gene-encoded amino acids by post-translational modification and was previously identified and characterized within an 82-residue subunit by chemical methods and crystallographic analysis at 2.05 Å resolution. It contains an orthoquinone moiety bound to the indole ring and catalyzes the oxidation of aliphatic and aromatic amines through formation of a Schiff-base intermediate involving one of the quinone O atoms. This paper reports the structural analysis of the complex of QHNDH with the enzyme inhibitor phenylhydrazine determined at 1.70 Å resolution. The phenylhydrazone product is attached to the C6 position, identifying the O6 atom of CTQ as the site of Schiff-base formation as postulated by analogy to another amine-oxidizing enzyme, methylamine dehydrogenase. Furthermore, the inner N atom closest to the phenyl ring of phenylhydrazine forms a hydrogen bond to γAsp33 in the complex, lending support to the hypothesis that this residue serves as the active-site base for proton abstraction during catalysis.

1. Introduction

The bacterium *Paracoccus denitrificans* contains two amine dehydrogenases, one being the well known tryptophan tryptophylquinone-containing methylamine dehydrogenase (Chen *et al.*, 1998) and the other a quinohemoprotein amine dehydrogenase (QHNDH) which is preferentially induced by growth on *n*-butylamine (Takagi *et al.*, 1999). The preferred substrates are medium-chain (three- or four-carbon) and aromatic amines and the enzyme is strongly and irreversibly inhibited by carbonyl compounds such as phenylhydrazine (Takagi *et al.*, 1999). The natural electron acceptor for QHNDH in this organism is cytochrome c_{550}, which mediates electron transfer to the cytochrome oxidase of the cytoplasmic membrane (Takagi *et al.*, 2001). QHNDH is a heterotrimer of 109 kDa molecular mass. The largest subunit (α) is 60 kDa and contains two heme *c* per molecule. The second subunit (β) is about 40 kDa. The smallest subunit (γ) is 9 kDa and stains positively for quinone-dependent redox cycling.

The crystal structure of QHNDH was determined at 2.05 Å resolution by the multiple isomorphous replacement method (Datta *et al.*, 2001). The α-subunit comprises four domains, one of which is a diheme cytochrome. The β-subunit is a seven-bladed β-propeller. The γ-subunit was found to contain a novel quinone-containing redox cofactor, cysteine tryptophylquinone (CTQ), consisting of a modified tryptophan side chain that is covalently linked to the S^{γ} atom of a cysteine side chain at position 4 of the indole ring. It also contains two

quinone O atoms bound to atoms 6 and 7 of the indole ring. This places QHNDH as a member of the rapidly growing class of proteins that contain post-translationally modified amino acids at their active sites (Okeley & Van Der Donk, 2000). The structure and nomenclature of the CTQ cofactor are shown in Fig. 1.

The CTQ cofactor is located in an internal cavity ~160 Å^3 in volume that is the probable binding site for substrate. The cavity is lined by hydrophobic and aromatic groups, about half of which are from the β-subunit and the remainder are from the γ-subunit. A large fragment of difference electron density within this cavity was modeled as *t*-butyl alcohol and another strong difference density peak nearby was modeled as a sodium ion.

In QHNDH, amine oxidation is believed to follow a ping-pong mechanism in which the quinone cofactor is reduced to an aminoquinol (the reductive half-reaction) and is then reoxidized by an electron acceptor to regenerate the oxidized quinone form of the cofactor (the oxidative half-reaction; Datta *et al.*, 2001). The reductive half-reaction proceeds through formation of a Schiff-base intermediate in which the imine N atom of the substrate replaces one of the quinone O atoms. This is followed by formation of a carbanion intermediate, leading to reduction of the cofactor through proton abstraction by a catalytic base on the enzyme. Based on analogy with methylamine dehydrogenase, also isolated from *P. denitrificans* and which also contains tryptophan tryptophylquinone as its redox cofactor (Chen *et al.*, 1998), O6 of CTQ (Fig. 1) is likely to be the site of attack by amine substrates, since O7 forms a strong hydrogen bond to a backbone amide group; furthermore, O6 is located close to the substrate analogue, *t*-butyl alcohol, in the native crystal structure. Also, the catalytic base was tentatively identified as γAsp33 because of its proximity to CTQ in the active site. However, the native structure did not provide definitive proof of the identity of the site of attack by substrate nor of the catalytic base. In this report, we describe the structure determination of the phenylhydrazone adduct of QHNDH (phz-QHNDH) at 1.7 Å resolution. This structure clearly identifies O6 of CTQ as the site of inhibitory attack by phenylhydrazine and identifies γAsp33 as a hydrogen-bond acceptor from one of the N atoms of phenylhydrazine. It also extends the resolution of the structure considerably beyond the initial value of 2.05 Å, thereby providing a more accurate structure of the enzyme.

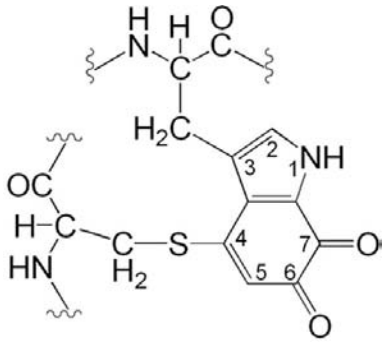

Figure 1
Chemical formula of the CTQ cofactor in QHNDH.

Table 1
Data-collection and refinement statistics.

Values in parentheses are for the highest resolution shell.

Data-collection statistics	
Wavelength (Å)	0.9
Resolution (Å)	30–1.70 (1.76–1.70)
Space group	$P4_12_12$
Unit-cell parameters	
a (Å)	99.24
c (Å)	213.06
No. of unique reflections	110131
R_{sym}†	6.0 (48.1)
Completeness (%)	94.2 (75.4)
Redundancy	6.7
$I/\sigma(I)$	27.7 (2.4)
Refinement and model statistics	
R/R_{free}‡ (%)	19.1/22.4
No. of protein atoms	6931
No. of non-protein atoms§	104
No. of water molecules	1295
B factors (Å^2)	
α-Subunit	22.6
β-Subunit	18.3
γ-Subunit	18.1
Non-protein atoms	17.8
Water molecules	33.4
R.m.s deviations	
Bonds (Å)	0.006
Angles (°)	1.4
ΔB factors, bonded atoms (Å^2)	
Main chain–main chain	0.7
Side chain–main chain	0.9
Side chain–side chain	1.3
Ramachandran plot¶	
Residues in most favored region	660 [86.6%]
Residues in additionally allowed region	95 [12.5%]
Residues in generously allowed region	3 [0.4%]
Residues in disallowed region	4 [0.5%]

† $R_{sym} = \sum |I_i - \langle I \rangle| / \sum I_i$, where I_i is the intensity of the *i*th observation and $\langle I \rangle$ is the mean intensity of the reflections. ‡ $R = \sum ||F_o - F_c|| / \sum |F_o|$, where F_o and F_c are the observed and calculated structure-factor amplitudes. R_{free} is calculated using 10% of reflections omitted from the refinement. § Includes two heme groups and four molecules of *t*-butyl alcohol. ¶ Analyzed using the program *PROCHECK* (Laskowski *et al.*, 1993). Glycine and proline residues are not included.

2. Methods and materials

Crystals of QHNDH were grown in the presence of sodium citrate (~100 m*M*, pH 5.6), PEG 4000 (~18%) and *t*-butyl alcohol (~21%) as described previously (Datta *et al.*, 2001). To prepare the complex with phenylhydrazine, the native crystals were soaked in a solution supplemented with 5 m*M* phenylhydrazine. The data were collected at 100 K on the BIOCARS beamline 14-BM at Argonne National Laboratory using an X-ray wavelength of λ = 0.9 Å. The data were processed using the *HKL* package (Otwinowski & Minor, 1997). The results of data collection and processing are given in Table 1.

The starting model for refinement was the structure of QHNDH previously determined at 2.05 Å resolution (Datta *et al.*, 2001). 10% of the reflections were set aside for cross-validation analysis by means of R_{free} (Brünger, 1992). Initial

rigid-body refinement was carried out using *CNS* (Brünger *et al.*, 1998) to an *R* factor of 26.3% using data in the 6.0–3.0 Å resolution range. The resolution was increased stepwise from 3.0 to 1.7 Å. After each step, $2F_o - F_c$ and $F_o - F_c$ electron-density maps were calculated and the model was rebuilt as necessary using *TURBO-FRODO* (Roussel & Cambillau, 1991). Water molecules were picked up from the difference map on the basis of the peak heights and distance criteria. A total of 1295 water molecules and four molecules of *t*-butyl alcohol were identified. 13 residues were refined in two alternate conformations and six proline residues are in the *cis* configuration. A summary of crystallographic refinement is given in Table 1.

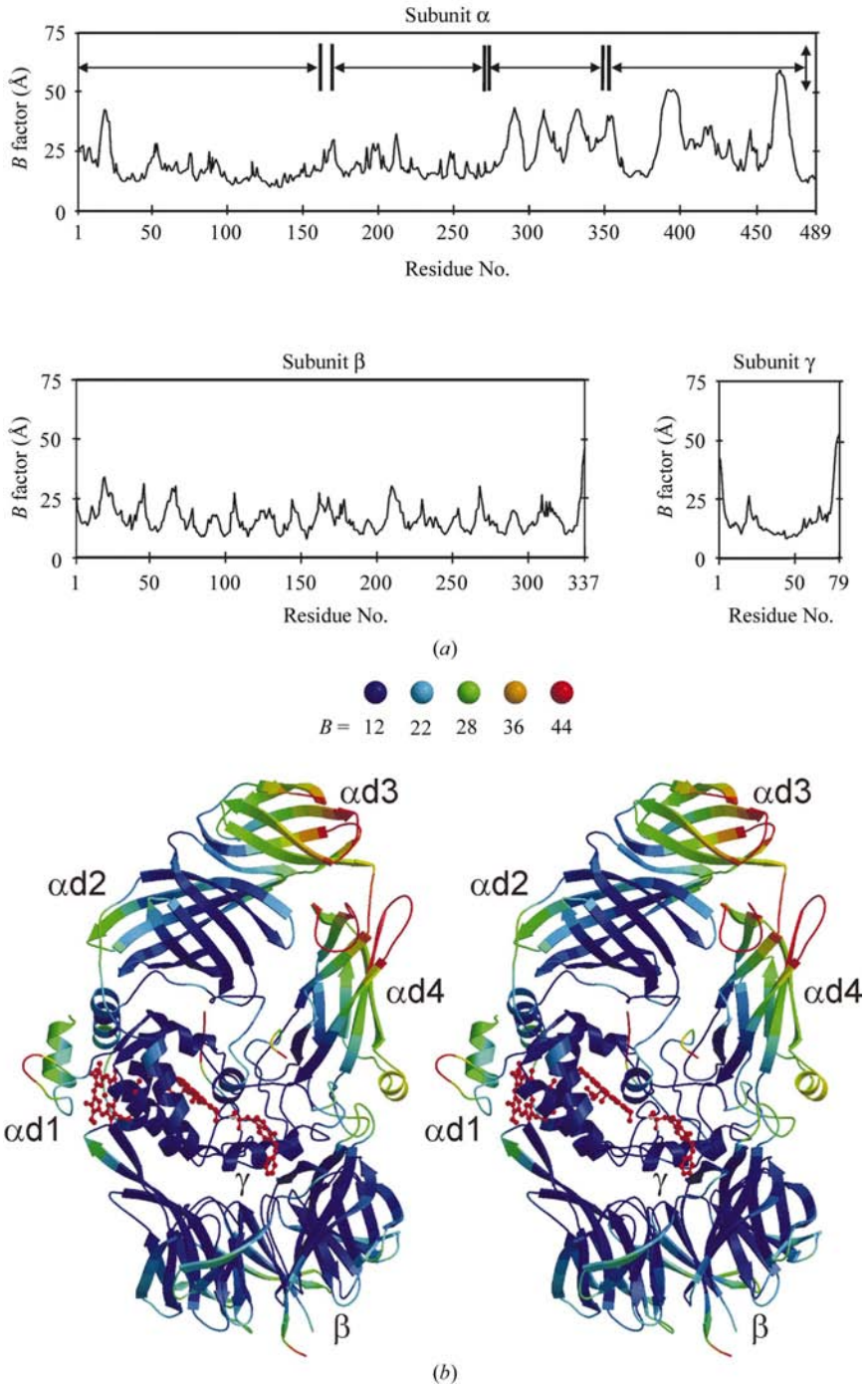

Figure 2
(*a*) Temperature-factor plot for the three subunits of phz-QHNDH averaged over all the atoms of each residue as a function of the residue number. The boundaries of the four domains of subunit α are also shown. (*b*) Stereo ribbon drawing of the three subunits of phz-QHNDH color-coded to indicate the average *B* factor of each residue. The *B*-factor color scale is indicated at the top of the diagram. The phz-CTQ adduct in the γ-subunit and the two heme groups of the α-subunit are drawn in red ball-and-stick representation. Subunits β and γ are labeled, as are the four domains of subunit α. This diagram was prepared using *MOLSCRIPT* (Kraulis, 1991) and *Raster3D* (Merritt & Bacon, 1997)

3. Results and discussion

3.1. Crystal structure analysis

The improved resolution (from 2.05 to 1.70 Å) obtained by the use of highly collimated and intense synchrotron radiation available at the Advanced Photon Source has enabled the entire structure of QHNDH to be better defined than previously for the native structure. All the residues in the structure could be located except the last three, residues 80–82, of the γ subunit. The average *B* factors for the β- and γ-subunits of phz-QHNDH (∼18 Å^2 each) are somewhat lower than that for the α-subunit (23 Å^2; Table 1). A plot of the *B* factors as a function of the residue numbers is given in Fig. 2(*a*) and the distribution of *B* values among the entire structure is shown in Fig. 2(*b*).

The residues in the active site of phz-QHNDH, including the phenylhydrazone adduct of CTQ, are very clearly defined in the final $(2F_o - F_c)$ electron-density map (Fig. 3*a*). At the end of the refinement, four features of electron density were found in the solvent region that could be modeled well as *t*-butyl alcohol and generally make van der Waals contact with one of more protein molecules in the unit cell. Two of these sites were reported in the 2.05 Å resolution native structure and the other two are compatible with the previous electron-density map, although not recognized. The previously reported *t*-butyl alcohol site within the active site, however, is displaced by phenylhydrazine (see below).

The number of residues in the disallowed region of the Ramachandran plot are reduced from six in the native structure to four (Table 1) and for each of these the electron density is very clearly defined. The strained conformation of each of these

residues appears to be stabilized by strong side-chain hydrogen bonding (αArg25), main-chain hydrogen bonding (βAla299) or both (βTyr159) with neighboring residues or by very bulky hydrophobic side-chain interactions (βLeu84). The configurations of the six *cis*-prolines that had been identified previously at 2.05 Å resolution in the native structure and are clearly defined in the present electron-density map. Two are in the α-subunit, two in the β-subunit and two in the γ-subunit. For one of these, γPro13, the less energetically favorable *cis* configuration may play a functional role in the protein, where main-chain atoms on either side of γPro13 form hydrogen bonds to CTQ (Fig. 3*a*). This and the tight packing of this highly irregular portion of the γ-subunit probably preclude adoption of the more common *trans* configuration normally observed for proline.

3.2. Overall structure

The crystal structure of phz-QHNDH is consistent with the native QHNDH structure determined earlier at 2.05 Å resolution (Datta *et al.*, 2001). phz-QHNDH is composed of three subunits (Fig. 2*b*). The 489-residue α-subunit is folded into four domains. The first domain (~167 residues) is a diheme *c*-type cytochrome containing four cysteine residues that are all involved in thioether linkages to the two heme groups. The other three domains are antiparallel or mixed β-barrel structures, the first having eight β-strands (~105 residues) and the other two having seven β-strands each. The β-subunit, a seven-bladed β-propeller of 337 residues, is folded as a single domain. The 82-residue γ-subunit is a highly cross-linked globular structure with little secondary structure. It is located above the β-subunit, with the CTQ nearly coincident with the sevenfold axis of pseudosymmetry of the β-propeller. The four domains of the α-subunit are wrapped around the γ-subunit, holding it in place in the center of the molecule. The γ-subunit also contains four cysteine residues, each of which is also involved in covalent carbon–sulfur thioether crosslinks, in this case to other amino-acid side chains within the γ-subunit. Two of these are to the β-carbon of aspartic acid, one to the γ-carbon of glutamic acid and one to tryptophan. The crosslink of greatest functional importance, between γCys37 and γTrp43, makes up part of the cysteine-tryptophylquinone (CTQ) redox cofactor, described above, (Fig. 1) in native QHNDH (Datta *et al.*, 2001).

In the α-subunit, the *B* factors are generally low for domains 1 and 2 (the diheme cytochromes and the eight-stranded β-barrel) and considerably higher for domains 3 and 4 (the two seven-stranded β-barrels) (Figs. 2*a* and 2*b*). The concave top surface of the β-subunit provides a base upon which the γ-subunit and the diheme cytochrome domain of the α-subunit rest (Fig. 2*b*). These three entities appear to form a rigid structure of catalytic importance for amine oxidation and electron transfer to other redox partners, while the remaining β-barrel domains of the α-subunit are more mobile and may be involved in other functions.

3.3. Phenylhydazine binding in the active site

The current structure of the phenylhydrazine derivative of phz-QHNDH very clearly defines the configuration and

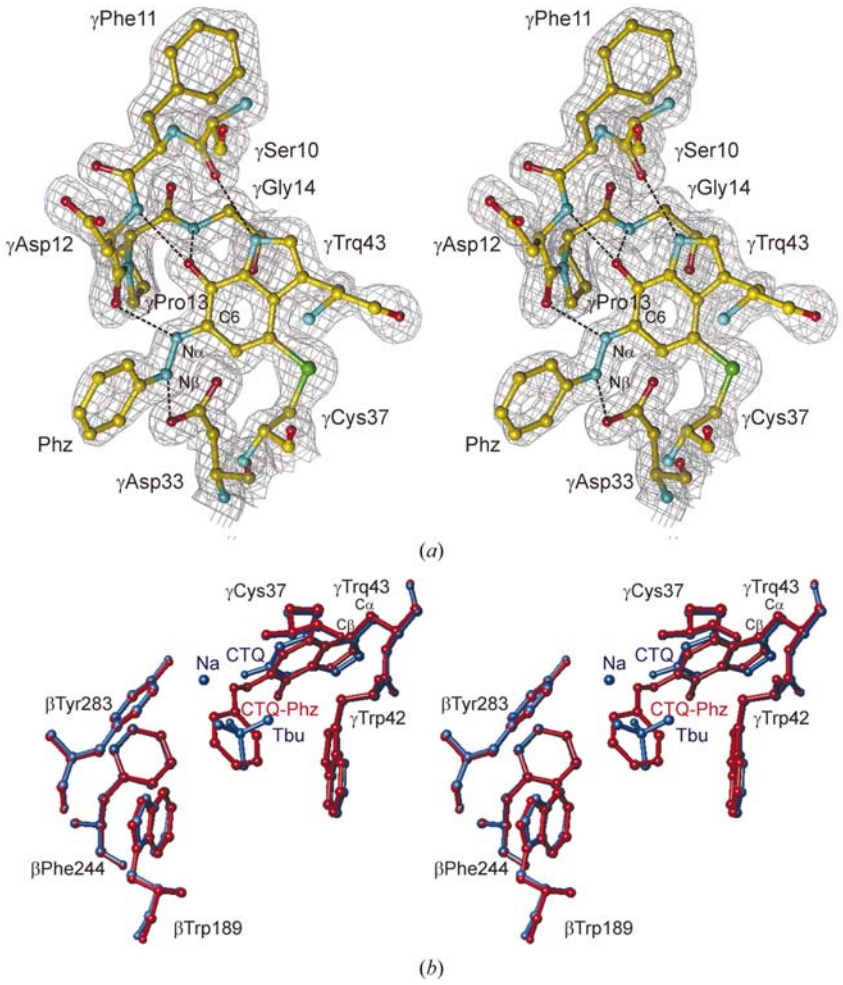

Figure 3
(*a*) Stereoview of the phenylhydrazine adduct of CTQ in phz-QHNDH superimposed on its electron density contoured at the 1.5σ level. The phenylhydrazine is bound to the C6 position as the hydrazone. The covalent link of Trq43 to Cys37 is also shown, as are the hydrogen bonds from phenylhydrazone and the Trq indole ring to residues Ser10, Asp12, Gly14 and Asp33 of the γ-subunit. The atoms C6, N^{α} and N^{β} of CTQ-phz are also shown. This diagram was produced using *TURBO-FRODO* (Roussel & Cambillau, 1991). (*b*) Stereo comparison of the structures of the active sites of the native (blue) and the phenylhydrazine adduct (red) of QHNDH. The bound phenylhydrazone of phz-QHNDH displaces the molecule of *t*-butyl alcohol and the sodium ion identified in the active site of the native enzyme. The only other structural difference between native and phz-QHNDH is a tilting of the indole ring of γTrq43 by about 11° upon binding phenylhydrazone. Atoms C^{α} and C^{β} of γTrq43, the axis of this rotation, are labeled. This diagram was produced using *TURBO-FRODO* (Roussel & Cambillau, 1991).

conformation of the CTQ cofactor and the bound phenylhydrazone adduct (Fig. 3*a*). The most important feature from the viewpoint of this study is the attachment site of the inhibitor at C6 of CTQ. Another important feature is the hydrogen-bonding pattern of interactions of the phenylhydrazine inhibitor and tryptophylquinone (Trq) side chain with the enzyme. The N^{α} atom of the phenylhydrazone donates a hydrogen bond to the carbonyl O atom of γAsp12 (2.6 Å) and the N^{β} atom donates a hydrogen bond to the carboxylate $O^{\delta1}$ of γAsp33 (2.8 Å), the putative active-site base. Atom O7 of Trq receives hydrogen bonds from the amide N atoms of γAsp12 (2.8 Å) and γGly14 (2.9 Å) and atom N1 of Trq donates a hydrogen bond to the carbonyl of γSer10 (2.9 Å). The phenyl ring of phenylhydrazone is nearly perpendicular to the indole ring of CTQ, with a dihedral angle between the two rings of about 100°.

The structural changes in CTQ resulting from inhibitor binding are limited (Fig. 3*b*). The phenyl ring of phenylhydrazone is accommodated in the hydrophobic cavity containing the active site, displacing the sodium ion and the *t*-butyl alcohol molecule found in native QHNDH. The only significant change in the QHNDH structure upon hydrazone formation is an 11° tilt of the indole ring of CTQ about its $C^{\alpha}-C^{\beta}$ bond and a concerted movement of the main and side chains of residues γThr10–γGly14 by about 0.5 Å (not shown). This concerted movement results in essentially no change in the hydrogen-bonding pattern of CTQ with the rest of the protein.

The chemical environment of the CTQ–phenylhydrazone adduct is shown in Fig. 4. Most of the hydrogen-bond interactions of CTQ within the γ-subunit are made with main-chain backbone atoms. In addition to the five hydrogen bonds described above, γTrq43 O forms hydrogen bonds with γGln46 N and γVal47 N and a water molecule bridges γTrq43 N and γCys37 O. Finally, the O and N atoms of γCys37 form hydrogen bonds with γTrp42 N and γAsp33 O, respectively. The environment also includes hydrophobic contact (defined as less than 4.0 Å) of the phenyl ring of phenylhydrazone with the side chains of βTrp189, βPhe244, βTyr283 and βLeu326 as well as with that of γTrp42.

The high-resolution structure of phz-QHNDH clearly identifies the C6 position of CTQ as the site of attack of the phenylhydrazine inhibitor. This confirms the earlier hypothesis (Datta *et al.*, 2001), based in part on tentative identification of *t*-butyl alcohol in the native enzyme active site, that the C6 of CTQ is the site of Schiff-base formation during the reductive half-reaction of the catalytic cycle of amine oxidation. In addition, the hydrogen bond formed by N^{β} of the phenylhydrazone with the side chain of γAsp33 provides additional evidence that the latter serves as the active-site base for proton abstraction during catalysis. This mechanism is similar to the proposed reaction mechanism of TTQ-dependent methylamine dehydrogenase (Chen *et al.*, 1998). Similar results have recently been described for the native and the *p*-dinitrophenylhydrazone adduct of a QHNDH isolated from *P. putida* (Satoh *et al.*, 2002, 2003).

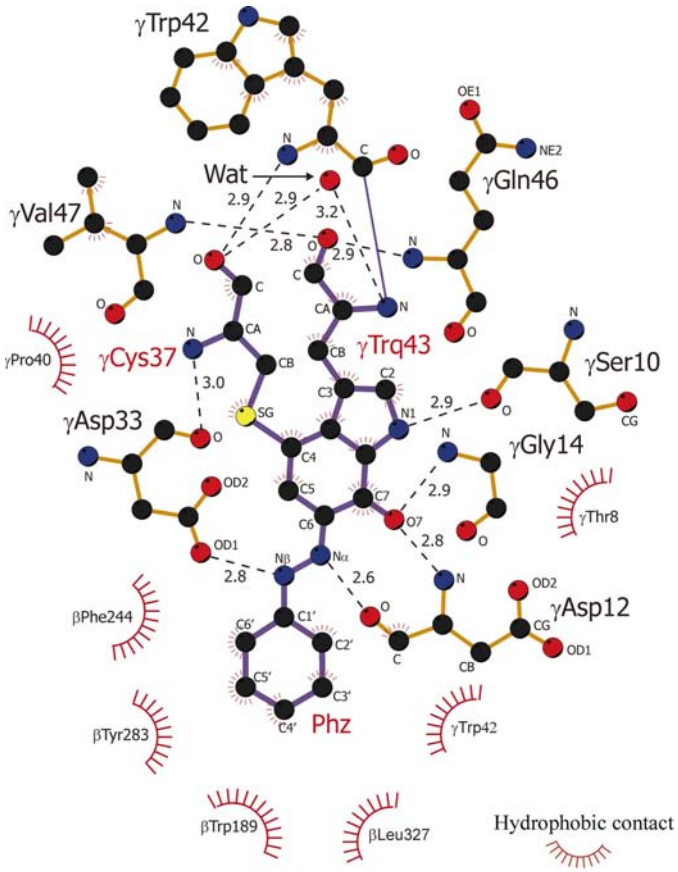

Figure 4
Schematic representation of the surroundings of CTQ and its phenylhydrazine adduct in phz-QHNDH. Hydrogen-bond distances are in Å. The single water molecule linking γTrq43 N with γCys37 O is shown. Residues making hydrophobic contact with CTQ or the adduct are indicated as shown at the bottom right. This diagram was prepared using the program *LIGPLOT* (Wallace *et al.*, 1995)

This work was supported by USPHS Grant No. GM31611 and NSF Grant No. MCB-0091084 (to FSM). Use of the Advanced Photon Source was supported by the US Department of Energy, Basic Energy Sciences, Office of Science under Contract No. W-31-109-Eng-38.

References

Brünger, A. T. (1992). *Nature (London)*, **355**, 472–475.
Brünger, A. T., Adams, P. D., Clore, G. M., Delano, W. L., Gros, P., Grosse-Kunstleve, R. W., Jiang, J. S., Kuszewski, J., Nilges, M., Pannu, N. S., Read, R. J., Rice, L. M., Simonson, T. & Warren, G. L. (1998). *Acta Cryst.* D**54**, 905–921.
Chen, L., Doi, M., Durley, R. C., Chistoserdov, A. Y., Lidstrom, M. E., Davidson, V. L. & Mathews, F. S. (1998). *J. Mol. Biol.* **276**, 131–149.
Datta, S., Mori, Y., Takagi, K., Kawaguchi, K., Chen, Z. W., Okajima, T., Kuroda, S., Ikeda, T., Kano, K., Tanizawa, K. & Mathews, F. S. (2001). *Proc. Natl Acad. Sci. USA*, **98**, 14268–14273.
Kraulis, P. J. (1991). *J. Appl. Cryst.* **24**, 946–950.
Laskowski, R. A., MacArthur, M. W., Moss, D. S. & Thornton, J. M. (1993). *J. Appl. Cryst.* **26**, 283–291.
Merritt, E. A. & Bacon, D. J. (1997). *Methods Enzymol.* **277**, 505–524.
Okeley, N. M. & Van Der Donk, W. A. (2000). *Chem. Biol.* **7**, R159–R171.

Otwinowski, Z. & Minor, W. (1997). *Methods Enzymol.* **276**, 307–326.
Roussel, A. & Cambillau, C. (1991). In *Silicon Graphics Geometry Partners Directory 86*, edited by Silicon Graphics. Mountain View, CA, USA: Silicon Graphics.
Satoh, A., Adachi, O., Tanizawa, K. & Hirotsu, K. (2003). *Biochim. Biophys. Acta*, **1647**, 272–277.
Satoh, A., Kim, J. K., Miyahara, I., Devreese, B., Vandenberghe, I., Hacisalihoglu, A., Okajima, T., Kuroda, S., Adachi, O., Duine, J. A., Van Beeumen, J., Tanizawa, K. & Hirotsu, K. (2002). *J. Biol. Chem.* **277**, 2830–2834.
Takagi, K., Torimura, M., Kawaguchi, K., Kano, K. & Ikeda, T. (1999). *Biochemistry*, **38**, 6935–6942.
Takagi, K., Yamamoto, K., Kano, K. & Ikeda, T. (2001). *Eur. J. Biochem.* **268**, 470–476.
Wallace, A. C., Laskowski, R. A. & Thornton, J. M. (1995). *Protein Eng.* **8**, 127–134.